

X-Ray Emission from Core Excitons

R. D. Carson and S. E. Schnatterly

Jesse Beams Laboratory of Physics, University of Virginia, Charlottesville, Virginia 22901

(Received 6 April 1987)

We have observed soft-x-ray emission from core excitons in several semiconductors and insulators and find that the exciton intensity is related to its binding energy. We propose an explanation for these excitons and this relationship using a Wannier model. The validity of the Wannier model is further tested by comparison of our measured exciton binding energies with predicted values. We conclude that this model appears to be a good starting point in the understanding of core excitons.

PACS numbers: 71.35.+z, 78.70.En

Core excitons in semiconductors and insulators have been studied theoretically¹ and experimentally²⁻⁶ with a number of models and measurement techniques. Despite extensive work, there remains considerable confusion about the most fundamental issues such as their size and binding energy, and whether a Frenkel⁷ or Wannier⁸ description is more appropriate. In this Letter we report measurements of a new property of core excitons—the intensity of the exciton as seen in soft-x-ray emission (SXE)—which we shall argue is relevant to these questions. The emission spectra also allow us to estimate the core-exciton binding energy in a new way, providing an important comparison with other techniques.

In SXE spectroscopy a core electron is removed from an atom and the emission spectrum is recorded as valence-band (VB) electrons make transitions into the core state. Ordinarily only occupied states are seen in emission. Sometimes a feature is seen above the VB at the core-exciton energy. We will discuss some reasons why this normally unoccupied state should be present in the spectrum. The intensity of the exciton peak is an intrinsic feature of the spectrum, being independent of the excitation electron current density and voltage over the ranges available to us.

Our spectrometer used electron-beam excitation and multichannel photodiode-array detection; details of the instrument are described elsewhere.⁹ The energy uncertainty and resolution ranged from 0.07 and 0.1 eV for Si *L* emission to 0.2 and 0.3 eV for C *K* emission. The samples included crystalline silicon, hydrogenated amorphous silicon, evaporated silicon, diamond, boron oxide, and boron nitride. The crystalline silicon was undoped and cleaved in air before mounting; the hydrogenated amorphous silicon was a film 8000 Å thick deposited on a Mo substrate by reactive sputtering; the evaporated silicon was a 2000-Å-thick film on a copper substrate; the diamond was a small gem-quality specimen; the boron oxide was a commercially available amorphous sample; the boron nitride was a highly oriented pyrolytic sample. The 3-kV excitation electron beam typically penetrates more than 1000 Å into the sample so that these measurements represent bulk properties. The data have been corrected for self-absorption by a procedure described by

Crisp.¹⁰ Shown in Fig. 1 are examples of the upper VB and core-exciton spectra for three samples.

The energies and exciton intensities were determined by fitting of the data with a simple model consisting of a straight line convoluted with a Gaussian for the VB edge, a Gaussian function for the exciton, and an underlying background. In the case of Si *L* emission a core-level spin-orbit splitting of 0.61 eV was used. Using this model we determined the VB edge (E_{VB}), the core-exciton energy (E_{CE}), and the exciton intensity normalized to the VB intensity (I_{ex}). Once we know the band gap (E_g), the exciton binding energy (E_{ex}) is then given by $E_{ex} = E_g - (E_{CE} - E_{VB})$. Table I lists these quantities and other relevant data for the samples. In the case of diamond, E_{ex} was obtained from a recent Elliot model

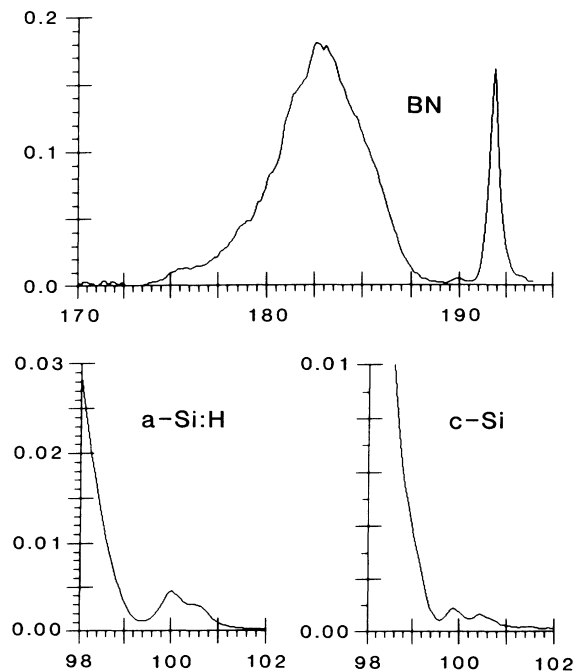


FIG. 1. Spectra showing the upper VB and core-exciton emission for three samples. All spectra have been normalized to give VB area of 1.

TABLE I. Energy of VB edge and core exciton, optical gap, effective mass, and dielectric constant for each sample. The last two columns give the exciton binding energy and exciton intensity.

Sample	E_{VB}	E_{CE}	E_g	μ	ϵ	E_{ex}	I_{ex}
c-Si	98.80	99.89	1.14 ^a	0.26 ^a	11.7 ^b	0.05 ± 0.02	$(2.2 \pm 0.5) \times 10^{-4}$
a-Si	98.57	99.86	1.4 ^c	...	13.1 ^c	0.11 ± 0.05	$(2.3 \pm 0.4) \times 10^{-3}$
C	0.48 ^d	5.7 ^b	0.19 ± 0.015^e	$(9 \pm \frac{1}{2}) \times 10^{-4}$
a-Si:H	98.52	100.00	1.75 ^f	...	12.6 ^f	0.27 ± 0.05	$(2.6 \pm 0.5) \times 10^{-3}$
B ₂ O ₃	188.0	193.9	6.7 ^g	...	2.21 ^h	0.8 ± 0.2	0.042 ± 0.005
BN	187.4	191.9	5.8 ⁱ	2.2 ^j	5.9 ^j	1.3 ± 0.2	0.12 ± 0.024
LiF	50.8 ^k	62.0 ^l	14.2 ^m	0.78 ⁿ	1.96 ^b	3.0 ± 0.3	0.42 ± 0.31^o

^aLandolt-Börnstein: Numerical Data and Functional Relationships in Science and Technology, edited by O. Madelung, M. Schultz, and H. Weiss (Springer-Verlag, Berlin, 1982), Group 3, Vol. 17.

^bHandbook of Optical Constants of Solids, edited by E. D. Palik (Academic, New York, 1985).

^cE. Freeman and W. Paul, Phys. Rev. B **20**, 716 (1979).

^dF. Nava *et al.*, Solid State Commun. **33**, 475 (1980).

^eReference 6.

^fT. Moustakas, private communication.

^gInelastic electron-scattering measurement in our laboratory.

^hCRC Handbook of Chemistry and Physics, edited by R. C. Weast (CRC, Boca Raton, FL, 1981).

ⁱA. Zunger, A. Katzir, and A. Halperin, Phys. Rev. B **13**, 5560 (1976).

^jReference 4.

^kS. P. Kowalczyk *et al.*, Phys. Rev. B **9**, 3573 (1974).

^lJ. R. Fields, P. C. Gibbons, and S. E. Schnatterly, Phys. Rev. Lett. **38**, 430 (1977).

^mM. Piacentini, C. G. Olson, and D. W. Lynch, Phys. Rev. Lett. **35**, 1658 (1975).

ⁿD. J. Mickish, A. B. Kunz, and T. C. Collins, Phys. Rev. B **9**, 4461 (1974).

^oReference 3; D. Ederer, private communication.

fit.⁶ Our E_{ex} values do not differ greatly from other recent determinations when they exist.⁵

Using SXE spectroscopy to measure simultaneously the VB edge and exciton position allows a more precise determination of E_{ex} than do other techniques. To date most such determinations have used x-ray photoemission spectroscopy (XPS) in which the VB edge and exciton energy were determined separately; E_{ex} is then evaluated as a small difference between two large energies and the combined errors often exceed the small difference. Furthermore, varying surface sensitivities of photoemission experiments together with surface core-level shifts have resulted in large discrepancies in E_{ex} as was pointed out by Margaritondo *et al.*¹¹ By use of SXE this surface sensitivity problem is avoided.

Shown in Fig. 2 is a log-log plot of I_{ex} vs E_{ex} for seven materials. I_{ex} covers a range of more than 3 orders of magnitude and E_{ex} nearly 2. The points fall close to a straight line with a slope of 2.1, suggesting that the intensity varies approximately as the square of E_{ex} . This large variation in intensity with E_{ex} is difficult to understand in a Frenkel exciton model in which the electron and hole are always in the same unit cell. Perhaps 1 order of magnitude intensity variation could occur as the binding energy of a Frenkel exciton is increased from 0 to 2 eV. This falls far short of explaining the intensity variation we observe.

In the Wannier model the exciton size and binding energy depend on material properties such as the dielectric constant and the effective mass. The exciton wave func-

tion can be written¹² as

$$\psi_{ex} = \sum_{\beta} e^{ia\mathbf{K} \cdot \beta} F(\beta) \Phi(\mathbf{K}, \beta), \quad (1)$$

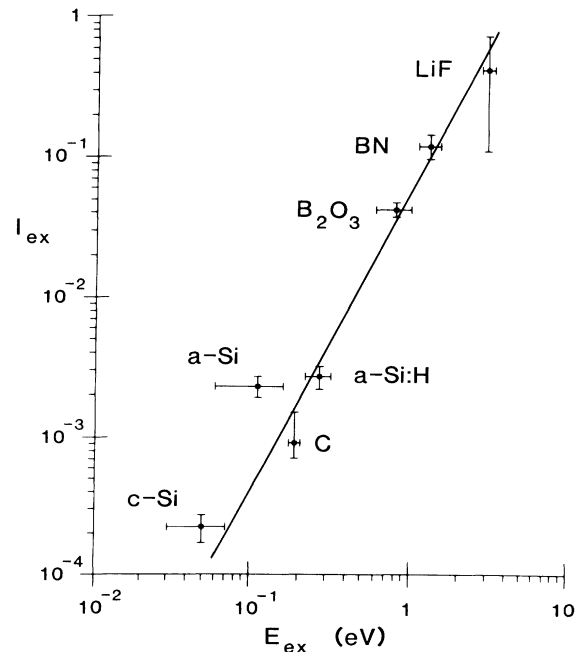


FIG. 2. Plot of exciton intensity vs binding energy for the samples. Intensity is defined in text. Line shows best fit and has a slope of 2.1 ± 0.2 .

where $\Phi(K, \beta)$ is an excited localized electron state centered on site β , \mathbf{K} is the wave vector, and $F(\beta)$ is the exciton envelope function normalized so that $|F(\beta)|^2$ is the probability that the electron is on site β . The core hole is located at site $\beta=0$. The radius of the envelope function (a_{ex}) and E_{ex} are related to the hydrogen atom Bohr radius (a_0) and Rydberg (R_H):

$$a_{\text{ex}} = \hbar^2 m_e / e^2 \epsilon_0 \equiv a_0 (\epsilon / \mu), \quad (2)$$

$$E_{\text{ex}} = e^4 \epsilon_0^2 / 2 \hbar^2 m_e \equiv R_H (\mu / \epsilon^2). \quad (3)$$

Here μ is the average effective mass at the bottom of the conduction band and ϵ is the dielectric constant at a frequency corresponding to E_{ex} .

Let P be the probability that a core hole traps an electron to form an exciton. From Eq. (1) we write the exciton intensity as

$$I_{\text{ex}} \equiv \frac{\text{exciton intensity}}{\text{VB intensity}} = \frac{|\langle \psi_{\text{core}} | x | \psi_{\text{ex}} \rangle|^2 P}{\sum_{\text{VB}} |\langle \psi_{\text{core}} | x | \psi_{\text{VB}} \rangle|^2} = M^2 F^2(0) P; \quad (4)$$

M is the ratio of the dipole emission matrix element of $\Phi(\beta=0)$ to that of the VB. We now consider each of the terms M^2 , $F^2(0)$, and P .

When a core hole is created the sudden change in potential can create plasmons and interband transitions which can be seen in XPS core spectra as satellites. The plasmons quickly decay via interband transitions producing more electron-hole pairs. Because these shakeup electrons are produced very quickly ($\approx 10^{-16}$ sec) and near the core hole they are available to form a core exci-

ton during the lifetime of the core hole ($\approx 10^{-14}$ sec). The integrated spectral intensity of shakeup structure is related to the VB electron density by a sum rule and does not vary much with material. Shakeup structure in XPS core-level spectra has been investigated theoretically¹³ and experimentally¹⁴ for many materials, some of which are included in this study. The overall shakeup probability is about 20%–30% for most materials. The number of resulting conduction electrons near the core hole will decrease as E_g increases. We therefore expect P to decrease somewhat as E_g increases.

When we compare the matrix element ratio [M^2 in Eq. (4)] for different materials some variation is again expected but this ratio increases with E_g , because of variations in the ionicity. For ionic materials the valence-electron density is higher on the anions while the exciton electron density is larger on the cations for the core excitons in this study. Thus we expect $M^2 \approx 1$ for homopolar semiconductors, with larger values for increasing ionicity. Although we expect both P and M^2 to vary with material, their product should not change greatly, certainly nothing like the observed variation in I_{ex} .

By the above arguments the exciton intensity variation should be dominated by the size of the envelope function [$F^2(0)$]. The exciton normalization requires that $F^2(0)$ vary inversely as the exciton volume so that $F^2(0) \sim a_{\text{ex}}^{-3}$; if we relate a_{ex} to E_{ex} using Eqs. (2) and (3) we will then have a relation between I_{ex} and E_{ex} . We seek a relationship which does not involve the material-dependent factors of ϵ or μ . But when Eqs. (2) and (3) are combined it is not possible to eliminate both ϵ and μ . Solving Eq. (2) for μ , $\epsilon^{3/2}$, or ϵ^2 and substituting into Eq. (3) yields

$$E_{\text{ex}} = \begin{cases} (R_H a_0 / \epsilon) a_{\text{ex}}^{-1}, \\ [R_H a_0^{3/2} (\epsilon \mu)^{-1/2}] a_{\text{ex}}^{-3/2}, \\ (R_H a_0^2 / \mu) a_{\text{ex}}^{-2}, \end{cases} \quad I_{\text{ex}} \propto a_{\text{ex}}^{-3} = \begin{cases} (\epsilon / R_H a_0)^3 E_{\text{ex}}^3, \\ (\epsilon \mu / R_H^2 a_0^3) E_{\text{ex}}^2, \\ (\mu / R_H a_0^2)^{3/2} E_{\text{ex}}^{3/2}. \end{cases} \quad (5)$$

In Eqs. (6) the product of ϵ and μ enters. This product is more nearly constant as one goes from one material to another than either ϵ or μ as in Eqs. (5) and (7). That this should be the case is reasonable. Roughly speaking the dielectric constant varies inversely with E_g , while the effective mass generally increases with E_g so that $\epsilon \mu$ should vary less than ϵ or μ alone as E_g changes. Equations (6) agree best with the observed relation between I_{ex} and E_{ex} . Using a Wannier model we can therefore achieve a qualitative understanding of our results.

As a further test of the Wannier model we plot E_{ex} vs μ / ϵ^2 in Fig. 3 which according to Eq. (3) should be a straight line of slope 1. The four samples in Table I for which both ϵ and μ are known lie along a line whose slope is nearly 1. The line shown corresponds to an average effective atomic Rydberg constant of 16 eV, somewhat larger than R_H . This is not unreasonable for core

excitons where central-cell corrections, dynamical screening, and other effects have been predicted to increase E_{ex} over the Wannier value.^{1,15}

When a cationic core hole is formed in a semiconductor or insulator, it frequently traps an electron to form a core exciton allowing the exciton to be seen in SXE. This conclusion by itself is new and may play an important role in other core properties. Our observed intensity-binding-energy relation can be qualitatively understood by use of a Wannier model and certain assumptions regarding the matrix elements and exciton formation. This result and our observed binding energies suggest that the Wannier model is a reasonable starting point for the study of core excitons. This appears to be so even though for BN, B₂O₃, and LiF the core excitons require a Frenkel description according to the usual cri-

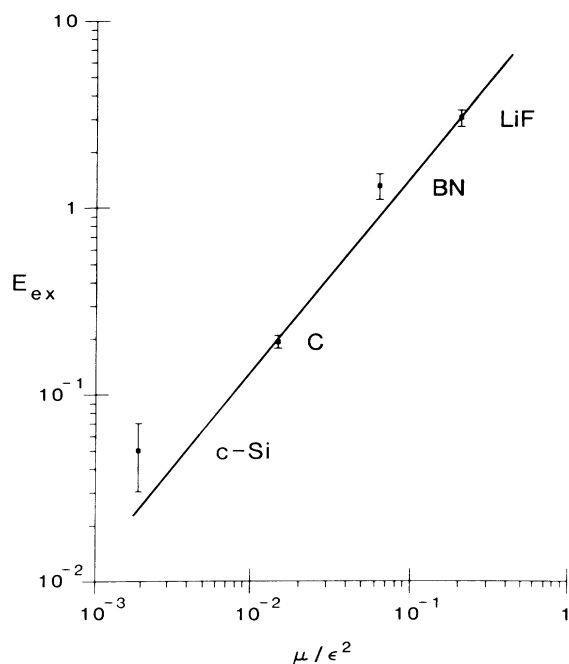


FIG. 3. Plot of E_{ex} vs μ/ϵ^2 for four samples. Slope is approximately 1 and intercept gives an average effective atomic Rydberg constant of 16 eV.

terion (a_{ex} less than the nearest-neighbor distance). Certainly most of the intensity variation shown in Fig. 2 is due to changes in $F^2(0)$ as described, but even for excitons normally considered to be Frenkel, the data points fall near the line. Thus the Wannier model is able to correlate the data well even when its validity is questionable. An explanation of this observation must await further theoretical work.

We would like to thank Ted Moustakas of Exxon and A. W. Moore of Union Carbide for their help in provid-

ing the α -Si:H and BN samples, respectively. We would also like to thank A. Mansour and C. Tarrío of our group for providing the data on the boron compounds and for absorption-coefficient data. Thanks also go to other members of our group—P. Bruhwiler, D. Husk, P. Livins, and J. Nithianandam—for their helpful suggestions and discussions. This research was supported under National Science Foundation Grant No. DMR-85-15684.

¹F. Bassani, *Appl. Opt.* **19**, 4093 (1980); F. Bechstedt, R. Enderlein, and M. Koch, *Phys. Status Solidi (b)* **99**, 61 (1980); H. Hjalmarson, H. Buttner, and J. Dow, *Phys. Rev. B* **24**, 6010 (1981); A. Quattropani *et al.*, *Nuovo Cimento B* **51**, 335 (1979).

²V. A. Fomichev, *Fiz. Tverd. Tela (Leningrad)* **9**, 3167 (1967) [*Sov. Phys. Solid State* **9**, 2496 (1968)].

³E. T. Arakawa and M. W. Williams, *Phys. Rev. Lett.* **36**, 333 (1976).

⁴B. M. Davies, F. Bassani, and F. C. Brown, *Phys. Rev. B* **24**, 3537 (1981).

⁵F. Evangelisti *et al.*, *Phys. Rev. Lett.* **53**, 2504 (1984).

⁶J. F. Morar *et al.*, *Phys. Rev. Lett.* **54**, 1960 (1985).

⁷J. Frenkel, *Phys. Rev.* **37**, 17 (1931).

⁸G. H. Wannier, *Phys. Rev.* **52**, 191 (1937).

⁹R. Carson *et al.*, *Rev. Sci. Instrum.* **55**, 1973 (1984).

¹⁰R. S. Crisp, *J. Phys. F* **13**, 1325 (1983).

¹¹G. Margaritondo *et al.*, *Solid State Commun.* **36**, 297 (1980).

¹²R. S. Knox, *Theory of Excitons*, Solid State Physics Supplement 5 (Academic, London, 1963).

¹³J. Chang and D. Langreth, *Phys. Rev. B* **5**, 3512 (1972); F. Bechstedt, *Phys. Status Solidi (b)* **112**, 9 (1982).

¹⁴L. Johanson and I. Lindau, *Solid State Commun.* **29**, 379 (1979); I. Ikemoto *et al.*, *Chem. Phys. Lett.* **38**, 467 (1976).

¹⁵G. Iadonisi and F. Bassani, *Nuovo Cimento D* **3**, 408 (1984); L. Resca and R. Resta, *Solid State Commun.* **29**, 275 (1979).